On addressable driving of 2D electrostrictive matrix

Eugene J. Danicki

***Abstract*—An analysis is presented for addressable driving of two-dimensional matrix transducer comprising crossed periodic metal strips on both sides of electrostrictive layer and representing the matrix rows and columns. Evaluation of stress in the layer excited by electrode potentials requires formulation of nontrivial electrostatic problem. Its solution and numerical examples are presented.**

***Index Terms*—transducer matrix, acoustic beam-forming.**

I. INTRODUCTION

Electrostrictive plates (ceramics or polymer membranes) find growing applications in actuators (*cf.* [1]–[3], for instance) and transducers [4], [5]. Typically, uniform electric field is applied to entire device causing its uniform deformation, as demonstrated in [6], [7]. Here, we discuss an arbitrary nonuniform electric field resulting in intentional nonuniform stress in the plate and its nonuniform vibrations. Transducers utilizing such electrode configuration were considered in literature recently [8], [9], although the concept was much earlier [10]. Perspective application of such a device may be in acoustic beam-forming transducers [11].

Consider a d-thick layer of dielectric permittivity ε with crossed periodic metal strips (electrodes) arranged on both sides of it, Fig. 1. Certain electric potentials (signals) drive each electrode: F_i and S_j on the bottom and upper sides of the plate, respectively, where i, j are the row and column numbers determining position of the (ij) matrix cell where the i, jth strips are crossing. Let the applied voltages F_i, S_j be the time-harmonic signals:

$$F_i = \cos 2\pi f_i t,\ S_j = \cos 2\pi (f_j - \Omega)t,\ f_l = l[MHz],\ \Omega \ll f_l, \quad (1)$$

in [kHz] range, for example (one may consider S_j shifted by an arbitrary phase ϕ_j). The resulting stress in the (ij)-cell is approximately [6]:

$$\sigma^{(ij)} = \varepsilon[(F_i - S_j)/d]^2 \sim 1 - \cos(f_i - f_j)t - \cos(f_i + f_j)t + \cdots . \quad (2)$$

In most applications the cell vibrations at high frequencies can be neglected, yielding the tool for selective (addressable) excitation of given cells: only this cell will vibrate with low frequency Ω, which resides between strips driven by signals F_i and S_j having frequencies different by Ω.

Let's consider another example, where $F_1 = \cos 2\pi f_1 t, F_2 = \cos 2\pi f_2 t$ (Fig. 1) and $S_1 = \cos 2\pi(f_1 - \Omega)t + \cos 2\pi(f_2 - \Omega)t, S_2 = \cos 2\pi(f_2 - \Omega)t$. One may check that only cells: $(11), (21)$ and (22) will vibrate at frequency Ω. Naturally, applying certain phase-shifts to S_j, amplitudes or different Ω's yields quite flexible tool for controlling vibrations of cells and the vibration distribution over an entire electrostrictive transducer matrix. The shape of vibrations requires detailed analysis of electric field distribution in the layer presented below.

E. Danicki is with Polish Academy of Sciences, Institute of Fundamental Technological Research, 5B Pawińskiego Str., Warsaw, 02-106 Poland, e-mail: edanicki@ippt.gov.pl.

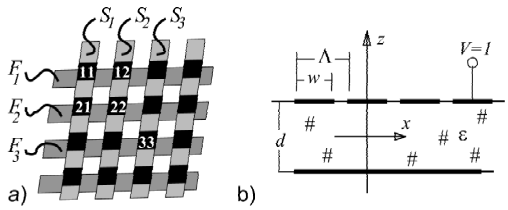

Fig. 1. a) Periodic metal strips (electrodes) arranged perpendicularly on both sides of electrostrictive layer and connected to external voltage sources. b) The voltage $V = 1$ is applied to the upper lth strip residing on a d-thick dielectric layer; other strips are grounded.

II. PLANAR ELECTRIC FIELD IN r-SPECTRAL DOMAIN

In this analysis, the known BIS-expansion method [12] is applied using the Bloch expansions for electric field on upper (superscript *u*) and bottom (superscript *b*) sides of the layer ($E = -\nabla\varphi, E_x, E_y$ are the tangential electric field and $D = D_z$ is the normal induction). Applying the pseudo-Einstein summation convention by neglecting the summation symbols over $m' \in [-M, M+1]$, $n' \in [-N, N]$, the expansions for strip period $\Lambda = 2\pi/K$ and width w are:

$$\begin{aligned}
D^u &= j\varepsilon \sum_{n',n,m} \alpha^m_{n'} P_{n-n'}(\Delta) e^{-jr_n x} e^{-js_m y}, \\
E^u_x &= \sum_{n',n,m} \alpha^m_{n'} S_{n-n'} P_{n-n'}(\Delta) e^{-jr_n x} e^{-js_m y} \\
D^b &= -j\varepsilon \sum_{n,m} \beta^n_{m'} P_{m-m'}(\Delta) e^{-js_m y} e^{-jr_n x}, \\
E^b_y &= \sum_{n,m} \beta^n_{m'} S_{m-m'} P_{m-m'}(\Delta) e^{-js_m y} e^{-jr_n x}, \\
K &= 2\pi/\Lambda,\ s_m = mK,\ r_n = r + nK,\ r \in (0, K)
\end{aligned} \quad (3)$$

where $\Delta = \cos Kw/2$ and P_k are the Legendre functions. These fields satisfy the boundary conditions stating that tangential field vanishes on strips and the normal induction vanishes between strips (neglecting the outside fields).

The unknown coefficients $\alpha^m_{n'}, \beta^n_{m'}$ are evaluated from the equations governing the field inside the layer presented in [12]; transformed here by applying the symmetry property $\beta^n_{1-m'} = \beta^n_{m'}$, they must be satisfied for any $n \in [-N, N-1]$ and $m \in [-M, 0]$, with $n' \in [-N, N], m" \in [-M, 0]$ and notation

$P_\nu = P_\nu(\Delta)$:

$$\begin{aligned}&\alpha_{n'}^m \left[S_{n-n'} \tanh k_{nm} d - \frac{r_n}{k_{nm}}\right] P_{n-n'} - \beta_{m"}^n \frac{r_n}{k_{nm}} \times \\ &\frac{P_{m-m"} + P_{-m-m"}}{\cosh k_{nm} d} = 0, \\ &\beta_{m"}^n \sum_{l=m,-m} \left[S_{l-m"} \tanh k_{nm} d - s_m / k_{nm}\right] P_{l-m"} - \alpha_{n'}^m \frac{s_\gamma}{k_n} \\ &\frac{P_{n-n'}}{\cosh k_{nm} d} = 0,\end{aligned} \tag{4}$$

where $S_\nu = \mathrm{sign}(\nu + 0)$ and $k_{nm} = \sqrt{r_n^2 + s_m^2}$ (note the symmetry $\alpha_{n'}^{-m} = \alpha_{n'}^m$). For $m = 0$, the last equation should be replaced by ($k = k_{nm}|_{m=0}$):

$$\begin{aligned}&-\frac{P_{n-n'}}{\cosh kd}\alpha_{n'}^0 + 2[(-1)^{m"} \frac{k}{K} \tanh kd \frac{d}{d\xi} \times \\ &P_{-m"+\xi}(-\Delta) \mid_{\xi=0} - P_{-m"}]\beta_{m"}^n = 0.\end{aligned} \tag{5}$$

The integration of electric field should yield the given strip potentials; for the assumed unitary voltage of lth upper strip and all bottom strips grounded, the condition results in (δ_{ij} is the Kronecker delta):

$$(-1)^{n'} \alpha_{n'}^m P_{-n'-r/K}(-\Delta) = \delta_{m0} \frac{K}{\pi} e^{jrl\Lambda} \sin \pi \frac{r}{K}. \tag{6}$$

Solving Eqs. (4), (5) and (6) for $\alpha_{n'}^M, \beta_{m'}^n$, the planar electric field on both sides of dielectric layer is determined by Eqs. (3). The system of equations becomes singular at $r = 0$ (consequently $E_x^u = 0$ and $D_z^u + D_z^b = 0$); to avoid this difficulty, $r = 10^{-6}K$ was applied instead in computed examples.

In principle, N, M involved in the above system of equations should be infinite, but practicaly it suffices to apply usually not very large finite numbers. Let N', M' be such that $\tanh N'Kd \approx \tanh M'Kd \approx 1$, then $N > N'$ should be chosen such that $r_N / k_{NM'} \approx 1$, and similarly for $M > M'$: $s_M / k_{N'M} \approx 1$. It can be checked that the solution to $\alpha_{n'}^m, \beta_{m'}^n$ changes negligible if N, M are chosen larger, except of being supplemented by close-to-zero components, meaningless for evaluation of electric fields from Eqs. (3). Properties saving the computation time are: $\alpha_{n'}^m(K - r) = [\alpha_{-n'}^m(r)]^*$ and $\beta_{m'}^n(K - r) = [\beta_{m'}^{-1-n}(r)]^*$.

III. Electrostrictive stress inside the layer

Integration of E^u given by Eqs. (3) over x for $y = 0$ (that is over the bottom strip center in this example) and subsequent inverse Fourier transformation over the spectral parameter r yields the potential spatial distribution at $z = d/2$ [13]:

$$\begin{aligned}\varphi(x) &= \frac{1}{K} \int_{-\infty}^{\infty} \frac{E_x^u(\rho)}{j\rho} e^{-j\rho x} d\rho \\ E_x^u(\rho) &= \sum_m \alpha_{n'}^m(r) P_{n-n'}(\Delta),\ n = \mathcal{E}(\rho),\end{aligned} \tag{7}$$

(for arbitrary y, replace $\sum_m \alpha_{n'}^m$ by $\sum_m \alpha_{n'}^m \exp(-jmKy)$), where $\mathcal{E}(\rho)$ is the closest integer smaller than ρ, thus $\rho = r + nK$ is the spectral parameter spanning an entire domain (using FFT, one has to truncate it in computations).

The charge distribution along the upper lth strip, that is the charge density integrated over the strip width, can be evaluated in similar manner:

$$\begin{aligned}Q_l(y) &= \sum_{m=-M}^{M} e^{-jmKy} \int_0^K Q_m(r) e^{-jrl\Lambda}\, dr/K, \\ Q_m(r) &= \int_{-\Lambda/2}^{\Lambda/2} D^u\, dx = j\varepsilon\Lambda\alpha_{n'}^m P_{-n'-r/K}(\Delta),\end{aligned} \tag{8}$$

from which one may evaluate the y-averaged mutual strip capacitances.

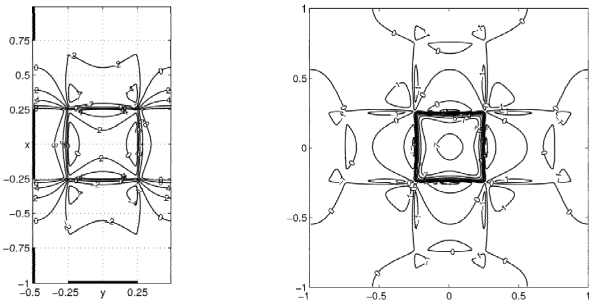

Fig. 2. Level maps of electric field (E_z, on the left) in the domain $2\Lambda \times \Lambda$ centered at $x = y = 0$, and the electostrictive stress σ (on the right) in the domain $2\Lambda \times 2\Lambda$ (*i.w.* axes are in Λ units), for $d/\Lambda = 0.15$, $w = \Lambda/2$.

As known [14], [15], the electric field is singular at the strip edges (this is the cost of idealization of real, finite-thickness electrodes by strips of infinitesimal thickness). In order to avoid the corresponding difficulty, we evaluate the electric field (in particular, its z-component) at the middle layer plane $z = 0$. This electric field can be reconstructed from the surface normal induction on both sides of the layer [12], again using spectral variable ρ and $n = \mathcal{E}(\rho), r = \rho - nK$:

$$\begin{aligned}&E_z(x,y) = 2\int_{-\infty}^{\infty} e^{-j\rho x} d\rho \times \\ &\sum_{m=-\infty}^{\infty} \frac{\alpha_{n'}^m(r) P_{n-n'}(\Delta) + \beta_{m'}^n(r) P_{m-m'}(\Delta)}{K \sinh(k_{nm} d/2)} e^{-jmKy}.\end{aligned} \tag{9}$$

Fast growing $\sinh(k_{nm}d/2)$ makes the above equation suitable for computation.

According to Eq. (2), stress $\sigma^{(ij)}$ (its z-component is considered only here) is proportional to the product of $E_z(x, y)$ resulting from the applied potential to the upper ith strip and $E_z(x, y)$ excited by the lower jth strip potential, which equals $E_z(y, x)$ in the considered case of the same strip periodicity and width. Fig. 2 presents numerical example of field distributions in relative scale: the maximum value of E_z is set to 10. It shows that the stress distribution is far from uniform and spans well outside the cell covered by the supplied strips.

IV. Conclusions

Detailed analysis of electrostatic field is presented for the recently proposed addressable driving of electrostrictive transducer matrix. Numerical examples show the electric field distribution and the resulting nonuniform stress induced in the area of the excited matrix cell (the code is available at *http://www.ippt.gov.pl/∼edanicki/CrosStrips.pdf*.

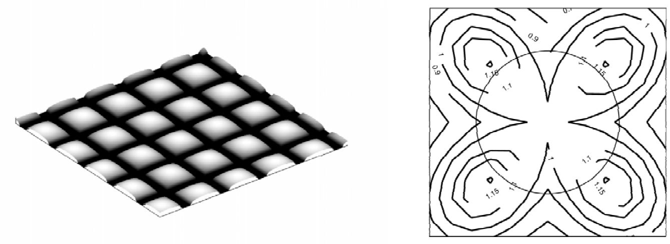

Fig. 3. Left: A proposed improvement to the transducer exploiting lateral expansion of the excited domain of electrostrictive foil (dark strips are fixed). Right: Spatial spectrum of the excited stress by two crossed strips.

It is well known that elastomer foils build their extend much their lateral dimension when electric field is applied to their thickness (*cf.* [7]). The structure sketched on the Fig. 5 (on left) may exploit well this property by forming the foil concave at the crossing domain of the upper and lower electrodes. Between them, the foil is fixed (attached to the solid frame), hence the excited concave domain must move upward when excited, producing pressure in the fluid to which the ultrasound is to be radiated.

The excited pressure (*ie.* the excited acoustic potential in the media) is not uniform over the excited transducer cell, and it extends over several neighboring cells as well. This may somehow distort the shape of the radiated wave-beam. In the paraxial approximation (*cf.* [16]), this shape corresponds to the spatial spectrum of the transducer pressure, shown in Fig. 3 (on right), taking into account that only central part of this spectrum, namely limited by the wave-number acoustic waves, can contribute to the wave-beam. This corresponds to the circle shown in the figure in the case of strip period equal half-wavelength of acoustic waves (the spectrum on the circle radiates in tangential direction to the transducer plane). One may see from the levels of the acoustic pressure presented in the figure remains flat within 15%, hence the wave-beam distortion in the discussed case may not be significant.

Acknowledgments. Author is indebted to Prof. P. Kiełczyński for help in search for references. Partial support by Ministry of Research and Higher Education under Grant No. N N518 3821 37 is acknowledged.

References

[1] A. Pimpin, Y. Suzuki, N. Kasagi, Micro electrostrictive actuator with metal compliant electrodes for flow control applications, *17 IEEE Int. Conf. MEMS 2004 Proc.*, Maastricht (2004), 478–481.

[2] R.E. Pelrine, R.D. Kornbluh, J.P. Joseph, Electrostriction of polymer with compliant electrodes as a means of actuation, *Sensors and Actuators A: Physical*, **64** (1998), 77–95.

[3] TRS Tehnologies, *http://www.trstechnologies.com/Materials/electrostrictive_ materials.php.*

[4] S. Sherrit, B.K. Mukherjee, Electrostrictive materials: Characterization and Applications for Ultrasound, *Proc. of SPIE* **3341** (1998), 196–207.

[5] A. Strachan, W.A. Goddard, Large electrostrictive strain at gigaherts frequencies on a polymer nanoactuator: Computational device design, *Appl. Phys. Lett.*, **86** (2005), 083103.

[6] S. Resset, M. Niklaus, P. Dubois, M. Dadras, H. Shea, Mechanical properties of electroactive polymer microactuators with ion implanted electrodes, *Proc. of SPIE*, **6524** (2007), 652410.

[7] C. Lynch, D. Brei, Z. Ounaies, M. Kamlah, S. Seelecke, S.D.E. Lucato, L. Weiland, *Smart Materials &, Structures. Adaptive and active materials: Selected papers from the ASME 2009 Conference on Smart Materials, Adaptive Structures and Intelligent Systems* Oxnard (2009).

[8] C.H. Seo, J.T. Yen, A 256x256 2-D array transducer with row-column addressing for 3D rectilinear imaging, *IEEE Trans. on Ultrasonics Ferroelectrics and Frequency Control*, **56** (2009), 837-847.

[9] I. Fujishima, Y. Tamura, H. Yanagida, J. Tada, Edge connected, crossed-electrode array comprising non-linear transducers, in *2009 IEEE International Ultrasonics Symposium Proceedings* (2009), 2221-2224.

[10] H.C. Schau, Edge-connected, crossed-electrode array for two-dimensional projection and beamforming, *IEEE Trans. Signal Proc.*, **39** (1991), 289–297.

[11] Y. Tasinkevych, Wave generation by a finite baffle array in application to beam-forming analysis, *Arch. Acoust.*, **35** (2010), 677–686.

[12] E. Danicki, Electrostatics of Crossed Arrays of Strips, *IEEE Trans. Ultras. Ferroelec. Freq. Control*, **67** (2010), 1701–1705.

[13] E. Danicki, *Spectral Theory of Interdigital Transducers*, available at http://www.ippt.gov.pl/∼edanicki/danickibook.pdf

[14] O.P. Thakur, A.K. Singh, Electrostriction and electromechanical coupling in elastic dielectrics at nanometric interfaces, *Material Science*, **27** (2009), 839–850.

[15] Q. Jiang, Z.B. Kuang, Stress analysis in two dimensional electrostrictive material with an elliptic rigid conductor, *Europ. J. Mech. A/Solids*, **23** (2004), 945-956.

[16] W.T. Cathey, *Optical Information Processing and Holography*, Wiley, New York 1974.